ChemPubSoc Europe

DOI: 10.1002/ejic.201601053

EurJIC European Journal of Inorganic Chemistry

Full Paper

Layered Compounds | *Very Important Paper* |

VIP

Structural Arrangement of 4-[4-(Dimethylamino)phenylazo]-pyridine Push–Pull Molecules in Acidic Layered Hosts Solved by Experimental and Calculation Methods

Klára Melánová,*[a][‡] Petr Kovář,[b] Martina Gamba,[b,c] Miroslav Pospíšil,[b] Ludvík Beneš,[d][‡] Vítězslav Zima,[a][‡] Jan Svoboda,[a][‡] David Miklík,[d] Filip Bureš,[d] and Petr Knotek[d]

Abstract: 4-[4-(dimethylamino)phenylazo]pyridine (further denoted as **G**) representing a type of push–pull molecules can be intercalated into α- and γ-modifications of zirconium phosphate (α-**ZrP** and γ-**ZrP**) and into zirconium (4-sulfophenyl)phosphonate (**ZrSPP**). The obtained intercalates form single phases with interlayer distances of 12.75, 16.31, and 24.11 Å for α-**ZrP**·0.2**G**·1.5H_2O, γ-**ZrP**·0.2**G**·1.5H_2O, and **ZrSPP**·0.5**G**·1H_2O, respectively. The increase of the interlayer distance upon intercalation suggests that the molecules of the intercalated guest lie parallel to the host layers. All intercalates were further characterized by IR and UV/Vis spectroscopy. The arrangement of the guests in the interlayer space was determined by molecular simulation methods. The calculations were performed separately for protonated and unprotonated forms of the guest in the models of hydrated and dehydrated α-**ZrP** and γ-**ZrP** intercalates. In the case of the α-**ZrP** intercalate, the presence of interlayer water stabilizes the head-to-tail arrangement of the guest molecules. Dehydration of this intercalate disturbs their arrangement, mainly in the case of protonated guest molecules. In the case of dehydrated γ-**ZrP**, the guest molecules are head-to-tail ordered, and the guest molecules in the hydrated form of γ-**ZrP** are more disordered than in the dehydrated intercalate. The simulations also describe a layer shift present in the dehydrated γ-**ZrP** intercalate, which explains why the rehydration of this intercalate is not possible.

Introduction

Photochemical and photophysical properties of dyes and chromophores can be modified by their intercalation into various layered host materials such as clays[1] or metal(IV) phosphates and phosphonates.[2] The cause for this change can be, among others, the modification of their immediate environment represented by a two-dimensional confined system of the host.[3] Chromophores of special interest from the point of their optical properties are those with a delocalized system of π-electrons end-capped with an electron donor (D) and an electron acceptor (A), widely known as push–pull systems.[4] A D–A interaction, or a so-called intramolecular charge transfer, is responsible for the polarization of the chromophore and generation of a molecular dipole. Organic molecules of this type show a second-order nonlinear optical (NLO) response that has attracted great interest thanks to their potential applications in electro-optic modulators and in wavelength conversion of lasers.[5]

Nevertheless, the main obstacle for their wide application is the fact that their assemblies or crystals usually have a center of symmetry that destructs their NLO properties.[6] One way to avoid the centrosymmetric arrangement of NLO active species is to incorporate them in a two-dimensional interlayer space of a layered compound.[7] It is supposed that under certain conditions the push–pull molecules spontaneously form a noncentrosymmetric arrangement in this environment. In an ideal case, a head-to-tail alignment of the push–pull molecules is created, in which all electric dipoles point to the same direction. One of such push–pull molecules is 4-[4-(dimethylamino)-α-styryl]-1-methylpyridinium (usually denoted as DAMS), which was intercalated into $MnPS_3$[8] and into α- and γ-modifications of zirconium hydrogen phosphate.[9] An azo analogue of DAMS, 1-methyl-4-[4-(dimethylamino)phenylazo]pyridinium, was intercalated into $MnPS_3$[8a,10] and layered metal oxalates[11] or prepared as hybrid nanoparticles with $MnPS_3$.[12] The optical properties of the prepared intercalates were investigated, and the relation between these properties and presumed arrangement of the intercalated molecules was discussed. We have recently reported how the nonlinear optical properties of NLOphores can be influenced by their intercalation into layered host materials.[13]

[a] *Institute of Macromolecular Chemistry, Academy of Sciences of the Czech Republic, Heyrovský Sq. 2, 16206 Prague 6, Czech Republic*
E-mail: klara.melanova@upce.cz
https://www.upce.cz/english/fcht/jlssch.html
[b] *Charles University, Faculty of Mathematics and Physics, Ke Karlovu 3, 12116 Prague 2, Czech Republic*
[c] *CETMIC–CCT La Plata, CICBA, Camino Centenario y 506, 1897 M. B. Gonnet, La Plata, Argentina*
[d] *Faculty of Chemical Technology, University of Pardubice, 53210 Pardubice, Czech Republic*
[‡] Present address: Joint Laboratory of Solid State Chemistry, Studentská 95, 53210 Pardubice, Czech Republic

Supporting information and ORCID(s) from the author(s) for this article are available on the WWW under http://dx.doi.org/10.1002/ejic.201601053.

The problem is that the arrangement of the guest molecules in these intercalates cannot be determined directly by experimental methods. Therefore, the question is whether it is possible on the basis of experimental data, such as the interlayer distance and the amount of intercalated chromophore, to model an arrangement of the push–pull molecules in the interlayer space of the host and thus predict optical properties of these materials. A suitable tool that might be used for the structure calculations are classical molecular simulations. In combination with the experimental methods [XRD, IR spectroscopy, thermogravimetry (TG) measurements] these simulations allow us to suggest the structure of the studied materials and to calculate the interactions between the guests and the host layers and between the guests themselves. This combination of theoretical and experimental methods can also help us to better understand the other properties of the intercalates and the relationship between structure and properties. From the molecular simulations point of view several papers dealing with the hybrid organo-inorganic materials based on zirconium hydrogen phosphates were published. These papers focused on mutual interactions of species, adsorption of guests, or pillaring properties.[14]

Several new compounds, in which 4-[4-(dimethylamino)-phenylazo]pyridine molecules are intercalated in acidic layered host materials [α-modification of zirconium hydrogen phosphate, γ-modification of zirconium hydrogen phosphate, and zirconium (4-sulfophenyl)phosphonate], were prepared and characterized. The main aim of this work is to describe the arrangement of the intercalated molecules of 4-[4-(dimethylamino)phenylazo]pyridine in α- and γ-modifications of zirconium hydrogen phosphate with a special focus on the question whether these flat-lying molecules could be arranged in a head-to-tail manner or not. This question is solved from the minimum energy point of view by using a combination of experimental data and molecular simulations.

Results and Discussion

The guest, 4-[4-(dimethylamino)phenylazo]pyridine, can be intercalated very easily into **ZrSPP** and γ-**ZrP**; the intercalates were obtained very simply by heating the host to reflux in an ethanol solution of the guest. In the case of α-**ZrP** such intercalation does not proceed, and the α-**ZrP·G** intercalate was prepared by mixing the exfoliated host with an ethanol solution of the guest.

The diffraction pattern of α-**ZrP·G** (see Figure S1 in the Supporting Information) contains two broad basal reflections corresponding to a basal spacing of 12.2 Å and several nonbasal reflections including those at 4.44 and 2.65 Å, which correspond to (200) and (020) diffraction lines of parent α-**ZrP** (JCPDS Nno. 04-016-8875).[15] The presence of these reflections in the diffraction pattern of the α-**ZrP** intercalate indicates that the structure of the host layers is not changed during the intercalation. After dehydration (Figure S1), the most intensive peak at 2θ = 7.23° (corresponding to the basal spacing of 12.2 Å) shifts to 7.36° (12.0 Å). Due to the generally low quality of the pattern it is difficult to assign the other peaks. The broadness of the basal reflections indicates that the particles of the intercalate formed are significantly smaller than that of the parent host (112 Å for α-**ZrP·G** compared to 382 Å for α-**ZrP**, as found by using the Scherrer formula). This is given by the methods of preparation of the intercalate through exfoliation. The dehydrated α-**ZrP·G$_D$** rehydrates back to the original hydrate as follows from its diffraction pattern.

In the case of the γ-**ZrP·G** intercalate (see Figure S2 in the Supporting Information), the diffraction pattern contains two basal reflections corresponding to a basal spacing of 16.3 Å, several broad weak reflections, and two intensive sharp reflections at 2θ = 26.9 (3.32) and 33.4° (2.68 Å), which correspond to (020) and (200) diffraction lines of parent γ-**ZrP** (JCPDS no. 04-012-1442).[15] After the dehydration (see diffraction pattern in Figure S2) the basal spacing of γ-**ZrP·G$_D$** is shifted from 16.3 to 14.6 Å. The peaks at 2θ = 26.9 and 33.4°, corresponding to (020) and (200) reflections found also in the parent γ-**ZrP**[15] and in the hydrated γ-**ZrP·G**, confirm that the structure of the host layers is retained both in the hydrated and dehydrated samples. In addition, new diffraction peaks appear in the diffraction pattern of the dehydrated intercalate at 2θ = 16.2 (5.48) and 22.6° (3.94 Å). These peaks might be an indication that the neighboring host layers are shifted to each other during the dehydration. This shift of the layers can be the reason for the stability of this dehydrated compound in a humid environment and impossibility of its rehydration back to γ-**ZrP·G**.

The diffraction pattern of the **ZrSPP·G** intercalate (Figure S3 in the Supporting Information) contains, besides four basal reflections corresponding to a basal spacing of 24.11 Å, a number of nonbasal reflections typical for the host structure. After the dehydration (see diffraction pattern in Figure S3 in the Supporting Information) the basal spacing of **ZrSPP·G$_D$** is shifted from 24.11 to 23.41 Å (calculated from 3 basal reflections), and the nonbasal reflections typical for the host structure are retained. The dehydrated **ZrSPP·G$_D$** rehydrates very slowly at high humidity; after 3 d, the basal spacing is 23.99 Å.

The composition of the intercalates was determined by elemental and TG analyses. All three intercalates decompose in two steps (see Figure 1). The TGA curves of both **ZrP** intercalates are nearly the same, which is in accordance with their composition found by elemental analysis. In the first step up to 200 °C, co-intercalated water is released. The observed weight loss of 8 %, corresponding to 1.5 molecules of water per formula unit, agrees well with the calculated values of 7.60 and 7.65 % for α-**ZrP·G** and γ-**ZrP·G**, respectively. The second step is caused by the decomposition of the intercalated guest. The end product of the decomposition is ZrP_2O_7 (JCPDS no. 04-008-5867)[15] in both cases. The total weight loss of 26.5 % is in accordance with the value of 25.4 % calculated for the presence of 0.2 guest molecules per formula unit. In the case of **ZrSPP·G**, the first weight loss corresponds to a release of one water molecule per formula unit (calculated value 2.66 %; found 3 %). The second weight loss is caused by the decomposition of the intercalated guest and the organic parts of the host. The end product of the thermal decomposition is again ZrP_2O_7. The total weight loss of 61 % agrees well with the value of 60.63 % calculated for the presence of half of the guest molecules per for-

mula unit. The thermogravimetric curves of the dehydrated intercalates have the same course as those of the hydrated intercalates above the temperature of dehydration.

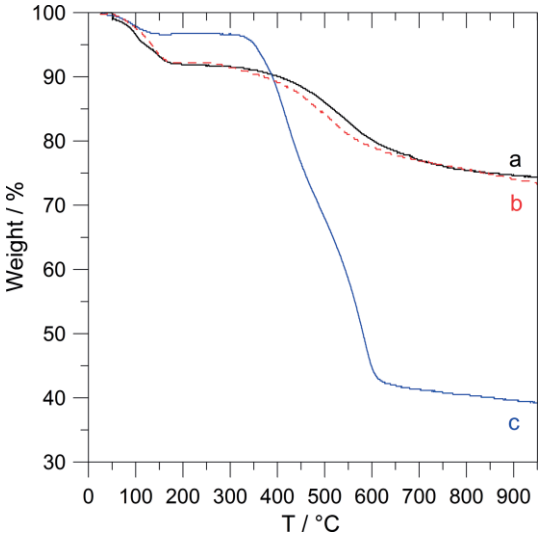

Figure 1. Thermogravimetric curves of the α-**ZrP·G** (a), γ-**ZrP·G** (b), and **ZrSPP·G** (c) intercalates.

The character of the interactions between the guest molecules and the host layers in the intercalates was studied by IR spectroscopy. In the spectrum of the pure guest, the bands at 3057 and 2868 cm^{-1} are probably caused by C–H stretching vibrations of the aromatic rings and the methyl groups, respectively. Four bands at 1605, 1583, 1522, and 1411 cm^{-1} [see Figure 2, curve (a)], corresponding to a ring stretching vibration of both benzene and pyridine rings,[16] were found in the spectrum. A strong band at 1367 cm^{-1} can be assigned to a C–N stretching vibration of the dimethylamino group bound to the benzene ring. A group of bands in the region from 1300 to 1000 cm^{-1} is probably caused by ring C–H deformation vibrations; the most intensive bands are at 1148 and 1067 cm^{-1}. A couple of bands at 834 and 823 cm^{-1} corresponds to an out-of-plane deformation of both rings.

In order to determine whether the guest compound is present in the intercalates in its protonated form, we recorded also the IR spectrum of its methylated analogue, 1-methyl-4-[4-(dimethylamino)phenylazo]pyridinium iodide. The spectrum of the pure methylated guest [see Figure 2, curve (e)] differs from the spectrum of **G** in the positions of the peaks of the ring stretching vibrations; there are several bands at 1632, 1605, 1567, and 1498 cm^{-1}. The positions of the bands of the ring C–H deformation vibrations are also affected by methylation on the N atom of the pyridine ring; the strong broad band with two maxima at 1061 and 1019 cm^{-1} appears, and also the position of the bands corresponding to an out-of-plane deformation of the ring changes slightly to 843 and 823 cm^{-1}. The sharp band corresponding to the C–N stretching vibration of the dimethylamino group was observed at the same position at 1367 cm^{-1}. In the IR spectra of all three intercalates [see Figure 2, curves (b), (c), and (d)], the most distinct feature is the broad band in the region of 1150–900 cm^{-1} belonging to the P–O vibrations of the host layers (and in addition to S–O vibrations in the case of **ZrSPP·G**). These bands are narrower in the spectra of the intercalates compared to the bands in the spectra of the parent hosts. The peaks of the δ_{P-OH} vibration, found in the spectra of α-**ZrP** and γ-**ZrP** at 1247 and 1218 cm^{-1}, respectively,[17] were observed also in the spectra of both intercalates. In the region of the ring stretching vibrations, bands at 1640, 1605, 1578, 1513, and 1470 cm^{-1} appeared. The shoulder at about 1620 cm^{-1} is probably caused by a δ_{H-O-H} deformation vibration of co-intercalated water. The IR spectra of all three intercalates in the region from 1800 to 600 cm^{-1} represent a superposition of the peaks found in the corresponding host and in the methylated guest, indicating that the guest molecules are at least partially protonated in the intercalates.

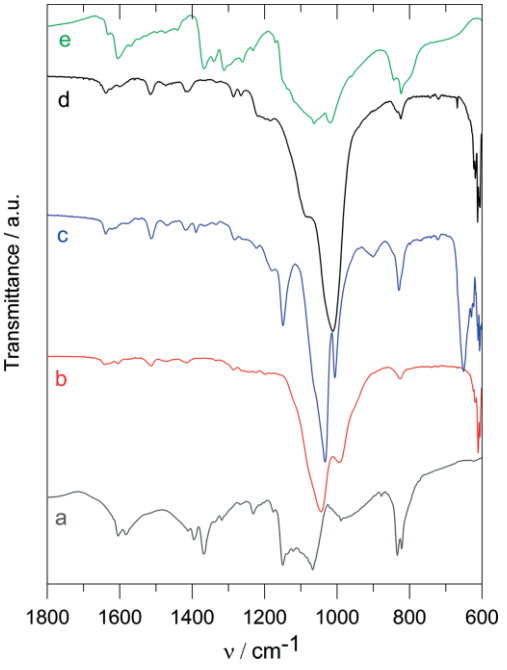

Figure 2. IR spectra of the pure guest (a), the α-**ZrP·G** (b), **ZrSPP·G** (c), γ-**ZrP·G** (d) intercalates, and the pure methylated guest (e).

UV/Vis Spectra

The UV/Vis spectra of the guest and the intercalates measured in the solid state are shown in Figure 3. The UV/Vis maximum for **G** is 440 nm, and the maxima for all intercalates are bathochromically shifted. The largest shift by 27 nm was observed for the γ-**ZrP·G** intercalate; a similar shift by 22 nm to 462 nm was found for α-**ZrP·G**. The lowest bathochromic shift was observed for the **ZrSPP·G** intercalate; the peak with the maximum at 443 nm is also the broadest one of all three intercalates. The IR spectra suggest that the guest is present in the intercalates in its protonated form. Therefore, the UV/Vis spectra of the intercalates were compared with those of an *N*-methylpyridinium analogue of the guest and the guest protonated by its exposure to HCl vapors. Quarternization of the pyridine N-atom by methylation of **G** causes a shift of the maximum in the UV/Vis spectrum by 110 nm, as can be seen from the comparison of curves (d) and (e) in Figure 3. On the contrary, only a small shift by

20 nm caused by the protonation of the guest molecule was observed [see curves (d) and (f) in Figure 3 for **G** and its protonated analogue, respectively]. The absorption peak of the protonated guest is sharper, and its FWHM is 82 nm, while it is 131 nm for the guest. The broadening and shift of the peaks of the intercalates might be caused by a coexistence of unprotonated and protonated forms of the guest molecules in the interlayer space of the host. The spectrum of α-**ZrP·G** shows a shoulder at the longer-wavelength side of the peaks. After the dehydration by heating up to 150 °C for 1 h, this shoulder disappears (see Figure S4 in the Supporting Information) and reappears again when the intercalate is rehydrated by exposure to an atmosphere with 75 % relative humidity at room temperature for 3 d. This shoulder at longer wavelengths is caused by a mutual interplay of the guest and water molecules. The presence of the water molecules decreases the mutual interactions between **G** and the host layers. This allows a regular head-to-tail arrangement of **G** and subsequently a formation of an ordered superstructure composed of **G** molecules, which is the reason for an existence of the shoulder at longer wavelengths in the absorption spectra. If we compare the results from the molecular modeling with a detailed description of azo-dye behavior in the literature,[18] we can assume that the shoulder for α-**ZrP·G** indicates a formation of a J-dimer-type arrangement of the guest species in the interlayer space of the host.

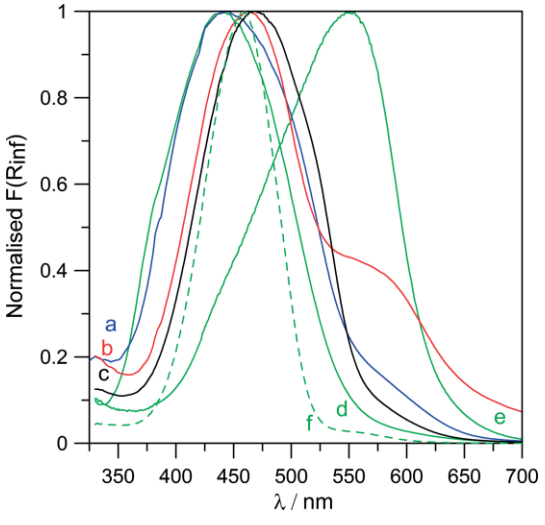

Figure 3. UV/Vis spectra of the **ZrSPP·G** (a), α-**ZrP·G** (b), and γ-**ZrP·G** (c) intercalates, the guest (d), the methylated guest (e), and the protonated guest (f).

Molecular Modeling

The arrangement of the guest molecules in the intercalates was modeled for compounds without water (dehydrated) and those containing water in the interlayer space. The volume available for the accommodation of the guest molecules in the interlayer space is smaller in γ-**ZrP·G** than in α-**ZrP·G**. In the case of α-**ZrP·G**, the surface area of the host layer ($3a \times 6b$ = 864 Å^2 per 6 guests) related to one guest molecule is about 30 % larger than that in the case of γ-**ZrP** ($6a \times 6b$ = 1286 Å^2 per 12 guests). Therefore, one can expect that the variability of the guest arrangement in the case of the γ-**ZrP·G** intercalate is limited.

In the case of the α-**ZrP** intercalate the supercell consisted of two host layers and two interlayer spaces, and every interlayer space contained 6 guest molecules. The supercell of the γ-**ZrP** intercalate consisted of one host layer and one interlayer space containing 12 guests.

Models of the Dehydrated α-ZrP Intercalate

The basal spacing of the dehydrated sample α-**ZrP·G$_D$** was 12 Å. Taking into account that the thickness of the layer in α-**ZrP** is 6.3 Å,[19] the height of the interlayer space (the so-called gallery height; see Figure 4a) is about 5.7 Å, which indicates a parallel or nearly parallel arrangement of the guest molecules in the interlayer space. The longitudinal axes of the guest molecules (as defined in Figure 4b) tend to be arranged in rows along the *b* cell vector (see Figure 5), keeping a head-to-tail arrangement. Mutual distances between the head (the N atom of the pyridine ring) and the tail (the nearest carbon atom of the dimethylamino groups of the neighboring guest) of the guest molecules are mostly between 4 and 5 Å. The distance between the guests (measured as a distance between their longitudinal axes, along the *a* cell vector) ranges mostly between 5 and 9 Å. In most cases the aromatic rings of the guests are in one plane, that is nearly no torsion along the N=N bond was observed. In the case of the protonated guest molecules (**G**$^+$), stronger mutual interactions between the guests and the charge-compensating host layers and between the guests themselves are present. This leads to a rather disordered arrangement of the guests in the interlayer space than in the case of unprotonated guest molecules. The longitudinal axes of the guests mostly do not tend to be in rows, and the guests are not in a head-to-tail arrangement.

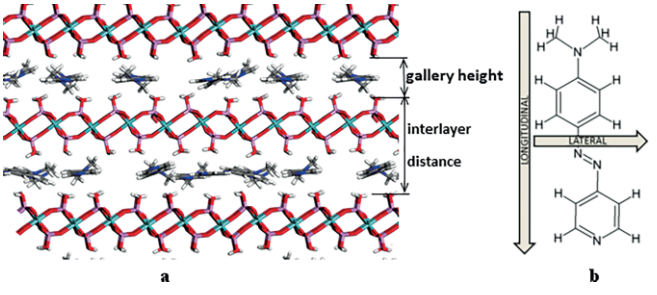

Figure 4. Side view of the interlayer arrangement of **G** in the α-**ZrP·G$_D$** intercalate (a). Longitudinal and lateral axes of the guest molecule (b).

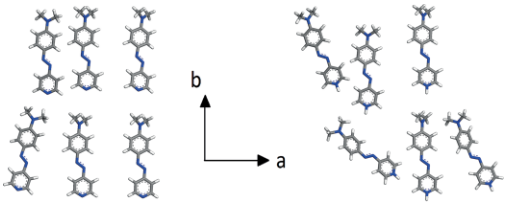

Figure 5. Top view of the guest arrangement (**G** left; **G**$^+$ right) in the interlayer space of the α-**ZrP·G$_D$** intercalate.

The basal spacing of the calculated models ranges from 11.7 (for **G**$^+$) to 12 Å (for **G**). If one takes into account the presence

of both **G** and **G**$^+$ in the interlayer space, the calculated basal spacing is in good agreement with the experimental data. The calculated X-ray diffraction pattern is compared with the experimental one in Figure 6. In contrast to the calculated XRD pattern, which contains sharp reflection peaks stemming from the supposed ideal crystal structure of the model, the experimental XRD profile contains poorly resolved peaks reflecting the poor crystallinity of the real sample. This makes it impossible to assign individual peaks in the experimental pattern to those calculated from the model.

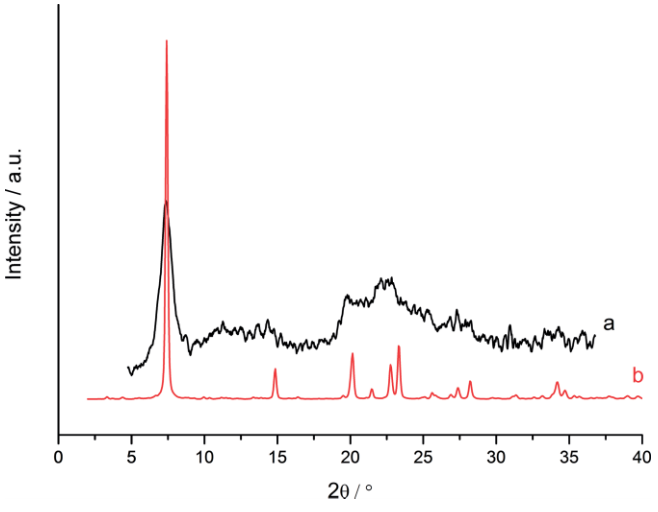

Figure 6. Experimental (a) and calculated (b) powder X-ray diffraction patterns of α-**ZrP·G$_D$**.

Models of the Hydrated α-ZrP Intercalate

The presence of water molecules in the interlayer space of α-**ZrP·G** led to an increase of the basal spacing from 12 to 12.2 Å. The calculated basal spacings are 12.1 and 12.2 Å for **G**$^+$ and **G** models, respectively. The longitudinal axes of the guests (for both **G** and **G**$^+$ molecules) tend to be arranged in rows and keep a head-to-tail arrangement (see Figure 7a and b). The guests in the interlayer space are distributed more evenly than in the case of the models without water. The distance between the longitudinal axes of the guests (in the direction of the *a* cell vector) ranges mostly between 8 and 10 Å for **G** and 8.6 and 9.6 Å for **G**$^+$. The distance between the head and the tail of the neighboring guest molecules in the *b* cell vector direction ranges mostly from 4 to 5 Å. The aromatic rings of the guests lie nearly in one plane: only a slight torsion around the N=N bond was observed.

As in the case of the models of the dehydrated compound, the guests can exhibit a certain degree of disorder. One can see that the guest planes tend to be parallel with the host layers, but in some cases their lateral axes (as defined in Figure 4b) adopt a tilted orientation (see Figure 8). The molecules of water are located in two positions: (i) near the host layers between the PO_4 tetrahedra (the water molecules interact with hydrogen atoms of the PO_4 tetrahedra through hydrogen bonds), and (ii) between the guests as a consequence of their hydrophobicity. From the comparison of the arrangements of the guests in the models without and with water we can conclude that the water molecules in the interlayer space stabilize the head-to-tail arrangement of the guests and lead to a more ordered arrangement in the interlayer space.

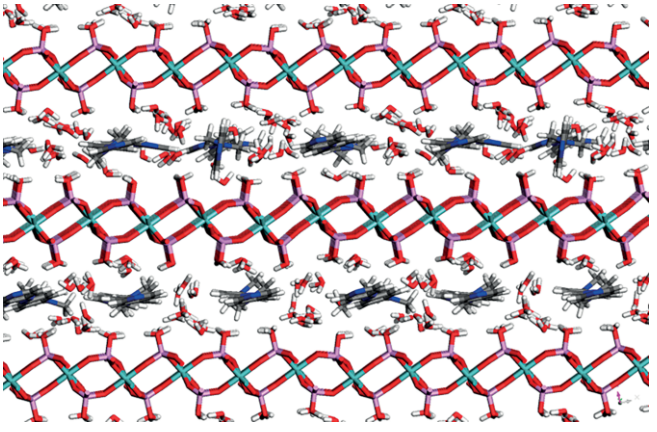

Figure 8. Side view of the arrangement of the **G** (**G**$^+$) molecules in the interlayer space of the hydrated α-**ZrP** intercalate.

Models of the Dehydrated γ-ZrP Intercalate

After the dehydration of γ-**ZrP·G**, new peaks at 2θ = 16.2 and 22.6° appear in the experimental powder X-ray pattern of the

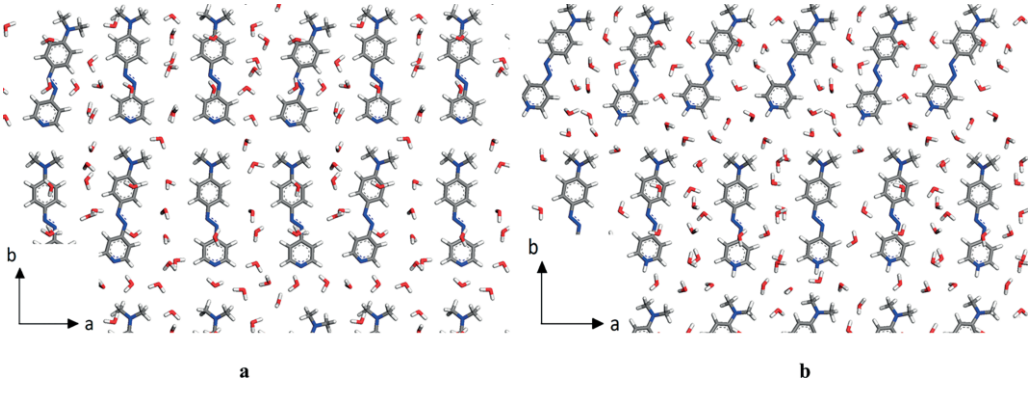

Figure 7. Top view of the arrangement of unprotonated guest molecules in α-**ZrP·G** (a) and protonated guest molecules in α-**ZrP·G**$^+$ (b).

product of dehydration, γ-**ZrP·G$_D$** (see Figure S2 in the Supporting Information and Figure 9a). These changes in the XRD pattern can be simulated by a shift of the layers by about 3 Å along the *b* cell vector, which is nearly half of the distance (6.6 Å) between the apexes of the neighboring PO_4 tetrahedra. In the γ-**ZrP·G** intercalate the apexes of the PO_4 tetrahedra are located between two neighboring tetrahedra apexes of the opposite layer (see Figure S5a in the Supporting Information). After the shift of the layers, the apexes of the PO_4 tetrahedra in one host layer of the γ-**ZrP·G$_D$** intercalate are above the apexes of the tetrahedra of the neighboring layer as shown in Figure S5b. The basal spacing of the calculated models ranges from 14.6 (for γ-**ZrP·G$_D$**$^+$) to 14.8 Å (for γ-**ZrP·G$_D$**) and is in good agreement with the experimental basal spacing of 14.6 Å. The simulated powder X-ray pattern (Figure 9b) then agrees quite well with the experimental one. On the other hand, when a model without shifted layers is used, its powder X-ray pattern (Figure 9c) does not correspond to the experimental pattern (Figure 9a).

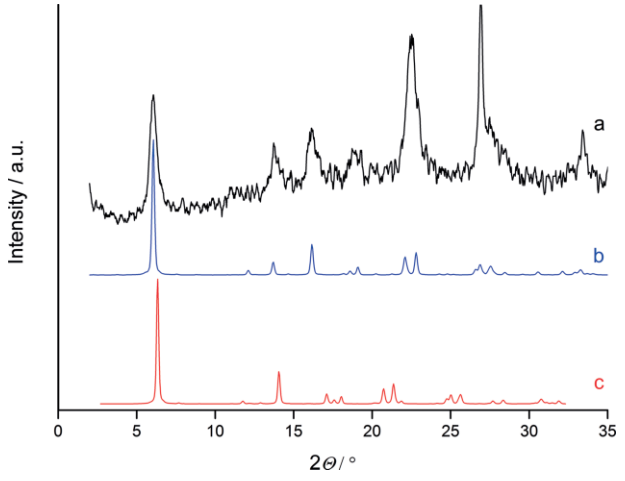

Figure 9. XRD patterns of the dehydrated γ-**ZrP** intercalate: experimental data (a), the models of γ-**ZrP·G$_D$** with shifted layers (b) and without shifted layers (c).

Figure 10a shows a view looking along the guest arrangement in the interlayer space of γ-**ZrP·G$_D$**. One can see an ordered head-to-tail arrangement of the guest molecules and their position with respect to the PO_4 tetrahedra of the "lower" host layer. The mutual distance between the longitudinal axes of guests in the *b* cell vector direction ranges between 6 and 7 Å. The head-to-tail distance of two neighboring guest molecules in the *a* vector direction ranges between 4.5 and 5 Å. The guests adopt a parallel arrangement with respect to the host layers. Due to a lower gallery height (4.3 Å) in comparison with α-**ZrP·G**, no guest molecules are tilted with respect to the host layers (see Figure 11a). The PO_4 tetrahedra form channels in the directions along the *a* and *b* lattice vectors due to the

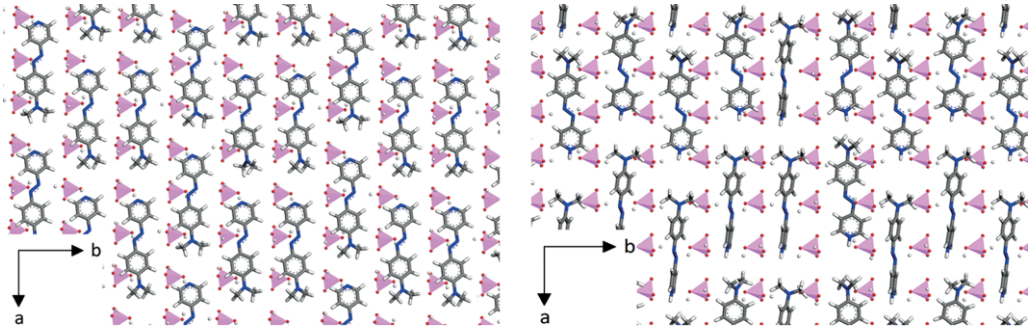

Figure 10. Top view of the interlayer arrangement of **G** in the γ-**ZrP·G$_D$** intercalate (a) and **G**$^+$ in the γ-**ZrP·G$_D$** intercalate (b). The violet tetrahedra are PO_4 groups of the "lower" host layer.

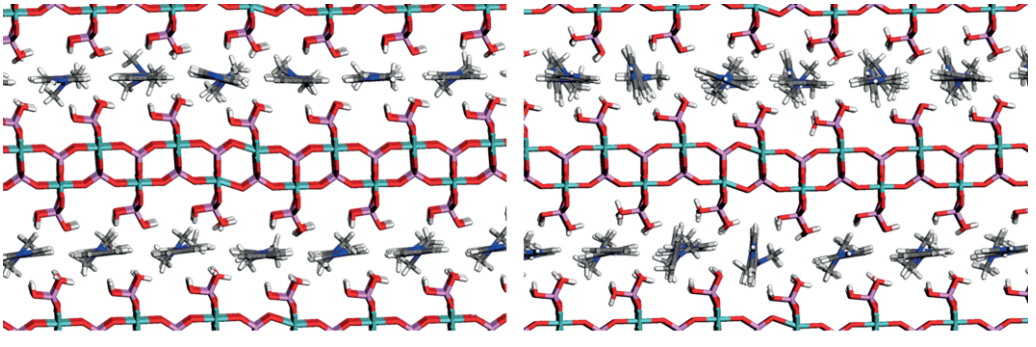

Figure 11. Side view of the interlayer arrangement of **G** in γ-**ZrP·G$_D$** (a) and **G**$^+$ in γ-**ZrP·G$_D$**$^+$ (b).

layer shift. The lower gallery height and the smaller interlayer area keep the guests in these channels; the methyl groups of the guests are located between the PO_4 tetrahedra. In the case of the γ-**ZrP·G**$^+$ model, the guest molecules adopt a very similar arrangement in the interlayer space as in γ-**ZrP·G**. The majority of the guest molecules exhibit a parallel arrangement with respect to the layers. The channels formed by the shift of the layers can theoretically accommodate the guests with their lateral axes perpendicular or nearly perpendicular with respect to the layers. We built a set of models where all guests were parallel with respect to the host layers and models where all lateral axes of the guests kept a perpendicular arrangement. While in the case of γ-**ZrP·G$_D$** all the guest molecules adopted a parallel arrangement, in γ-**ZrP·G$_D$**$^+$ some of **G**$^+$ retained a perpendicular arrangement, most probably due to a mutual repulsion of the **G**$^+$ cations (see Figure 10b and Figure 11b).

Models of the Hydrated γ-ZrP Intercalate

Presence of the interlayer water led to an increase of the basal spacing from 14.6 to 16.3 Å. The calculated basal spacing of 16.1 Å for both γ-**ZrP·G** and γ-**ZrP·G**$^+$ is in good agreement with the experimental value.

The increase of the gallery height led to the following differences in the guest arrangement in comparison with the models without water: (i) Even if the longitudinal axes of the guest molecules **G** are parallel with the plane of the host layers, their lateral axes are not (see Figure 12a). Most of the guest molecules keep a tilted orientation of the lateral axis with respect to the layers, and the angle, under which they are tilted, ranges from 20 to 30°. The **G**$^+$ cations also adopt a tilted orientation, but they are arranged randomly with respect to each other and form a disordered arrangement (see Figure 12b). (ii) The guest molecules tend to be located in the channels formed by the PO_4 tetrahedra, but their arrangement within them is not ordered as that in the models of the dehydrated intercalate. In the case of γ-**ZrP·G**$^+$ some of the guests are not located in the channels at all due to mutual repulsive interactions. Water molecules in both protonated and unprotonated models are located in two positions: (i) between the apexes of the host layer tetrahedra (most of them) and (ii) between the guest molecules.

Conclusions

A typical representative of a push–pull molecule, 4-[4-(dimethylamino)phenylazo]pyridine, was intercalated into three acidic layered host materials, namely the α-modification of zirconium phosphate, the γ-modification of zirconium phosphate, and zirconium (4-sulfophenyl)phosphonate. The interlayer distance of all three intercalates suggests that the guest molecules are arranged with their longitudinal axes parallel to the host layers.

The arrangement of the guests in the intercalates with both modifications of zirconium phosphate was investigated with use of molecular simulations. Molecular simulations in combination with X-ray diffraction patterns provided an insight into the interlayer arrangement of the guests including the role of interlayer water. In the case of α-**ZrP·G** intercalate, the presence of interlayer water stabilizes the head-to-tail arrangement of the guest molecules. Dehydration of this intercalate leads to disruption of their arrangement, mainly in the case of the protonated guest molecules. In the case of γ-**ZrP·G$_D$**, the guest molecules are head-to-tail ordered; protonation of the guest leads only to tilting of their lateral axes. On the other hand, the guest molecules in γ-**ZrP·G** are more disordered than those in the dehydrated intercalate. The suggested differences in the ordering of the guest molecules in the interlayer space of the hosts is in good agreement with the differences observed in the powder X-ray diffraction patterns. In α-**ZrP·G** with better-ordered guest molecules, the diffraction peaks are more pronounced than in the less-ordered dehydrated α-**ZrP·G$_D$** sample. Furthermore, in the case of γ-**ZrP** the powder X-ray diffraction pattern with more distinguishable peaks is that of γ-**ZrP·G$_D$**, where the guest molecules are better arranged than in γ-**ZrP·G**. The simulations also described a layer shift present in the dehydrated γ-**ZrP** intercalate (γ-**ZrP·G$_D$**), which is the reason why the rehydration of the γ-**ZrP·G$_D$** is not possible. Based on the presented calculated data, the α-**ZrP·G** intercalate seems to be a suitable material for applications in nonlinear optics.

Experimental Section

Synthesis of the Host Materials: Well-crystallized α-modification of $Zr(HPO_4)_2{\cdot}H_2O$ (further denoted as α-**ZrP**), was obtained according to the method proposed by Alberti and Torracca,[20] and γ-modification of $Zr(PO_4)(H_2PO_4){\cdot}2H_2O$ (further denoted as γ-**ZrP**) was

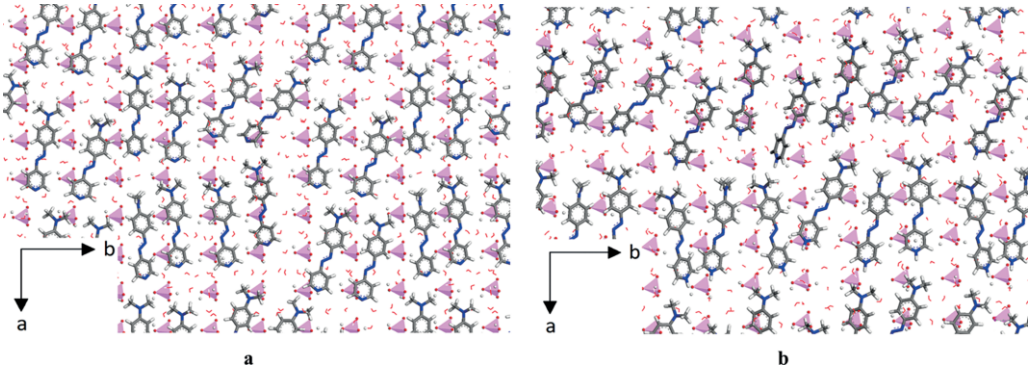

Figure 12. Top view of the interlayer arrangement of **G** in γ-**ZrP·G** (a) and **G**$^+$ in γ-**ZrP·G**$^+$ (b). The violet tetrahedra are PO_4 groups of the "lower" host layer.

obtained according to Poojary et al.[21] Zirconium (4-sulfophenyl)-phosphonate with the formula $Zr(HO_3SC_6H_4PO_3)_{1.8}(C_6H_5PO_3)_{0.2}\cdot 2H_2O$ (further denoted as **ZrSPP**) was prepared according to the procedure described by Zima et al.[22] The powder diffraction patterns (see Figures S1–S3 in the Supporting Information) show that the crystallinity of all prepared host compounds is quite good.

4-[4-(Dimethylamino)phenylazo]pyridine (G): The target guest compound (further denoted as **G**) was prepared by a modified Faessinger method[23] (see Scheme 1). Sodium nitrite (1.6 g, 23 mmol) was slowly added to a stirred solution of 4-aminopyridine (2 g, 21 mmol) in HBF_4 (15 mL) cooled to –15 °C, and the temperature was kept below –10 °C. The reaction mixture was stirred for additional 30 min, whereupon *N*,*N*-dimethylaniline (5.2 mL, 41 mmol) was added in one portion. The reaction mixture was stirred for 2 h and alkalized with a concentrated solution of sodium hydroxide. The resulting precipitate was filtered, washed with water (until the filtrate showed neutral pH) and subsequently washed with hexane (30 mL). The crude product was purified by column chromatography (SiO_2; $CHCl_3/Et_2O$, 3:1) to give the title compound as a bright orange solid: Yield: 3.8 g (80 %). M.p. 205.5–206.5 °C (207–209 °C[23]). ^{1}H NMR (500 MHz, 25 °C, $CDCl_3$): δ = 3.10 [s, 6 H, $N(CH_3)_2$], 6.72 (d, ^3J = 9 Hz, 2 H, Ar*H*), 7.62 (d, ^3J = 5.5 Hz, 2 H, NPy*H*), 7.89 (d, ^3J = 9 Hz, 2 H, Ar*H*), 8.70 (d, ^3J = 5.5 Hz, 2 H, NPy*H*) ppm. ^{13}C NMR (125 MHz, $CDCl_3$, 25 °C): δ = 40.30, 111.41, 116.06, 126.00, 143.51, 151.04, 153.33, 158.00 ppm. EI-MS: *m*/*z* (%) = 226 (100) [M^+], 148 (25), 120 (87), 105 (30), 77 (28), 51 (16).

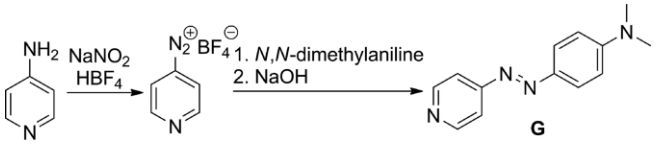

Scheme 1.

4-[4-(Dimethylamino)phenylazo]-1-methylpyridinium Iodide: A solution of the target guest compound **G** (226 mg, 1 mmol) in acetone (3 mL) and iodomethane (3 mL, 9.2 mmol) was stirred at room temperature for 12 h. The purple precipitate was filtered, washed with hexane, and dried under vacuum. Yield: 331 mg (90 %). ^{1}H NMR (400 MHz, 25 °C, [D_6]DMSO): δ = 3.21 [s, 6 H, $N(CH_3)_2$], 4.33 (s, 3 H, NPyCH_3), 7.03 (d, ^3J = 8.8 Hz, 2 H, Ar*H*), 7.98 (d, ^3J = 8.8 Hz, 2 H, Ar*H*), 8.17 (d, ^3J = 6.0 Hz, 2 H, Py*H*), 8.94 (d, ^3J = 6.0 Hz, 2 H, Py*H*) ppm. ^{13}C NMR (100 MHz, 25 °C, [D_6]DMSO): δ = 40.28, 46.83, 112.73, 118.19, 125.23, 143.64, 146.68, 155.62, 160.99 ppm.

Intercalation into α-ZrP: Compound α-**ZrP** (0.15 g) was exfoliated according to the procedure described by Zhou et al.[24] An ethanol solution (10 mL) of the guest (0.1 g) was added to this exfoliated host and shaken at room temperature for 5 d. The product (α-**ZrP·G**) was separated by centrifugation, extracted with a Soxhlet extractor until the extract was colorless, and dried in air. α-**ZrP·G** $[Zr(HPO_4)_2\cdot 0.20(C_{13}H_{14}N_4)\cdot 1.5H_2O]$ (355.46): calcd. C 8.79, H 2.21, N 3.15; found C 10.89 ± 0.02, H 2.51 ± 0.02, N 2.83 ± 0.02.

Intercalation into γ-ZrP and ZrSPP: The host (0.1 g) in ethanol solution (10 mL) of the guest (0.1 g) was heated to reflux for 8 h. The products (further denoted as γ-**ZrP·G** and **ZrSPP·G**) were separated by centrifugation, extracted with a Soxhlet extractor until the extract was colorless, and dried in air. γ-**ZrP·G** $[Zr(PO_4)(H_2PO_4)\cdot 0.19(C_{13}H_{14}N_4)\cdot 1.5H_2O]$ (353.20): calcd. C 8.40, H 2.19, N 3.01; found C 8.63 ± 0.03, H 2.02 ± 0.01, N 2.79 ± 0.01. **ZrSPP·G** $[Zr(HO_3SC_6H_4PO_3)_{1.8}(C_6H_5PO_3)_{0.2}\cdot 0.50(C_{13}H_{14}N_4)\cdot H_2O]$ (678.65): calcd. C 32.74, H 2.82, N 4.13, S 8.51; found C 30.95 ± 0.02, H 2.49 ± 0.01, N 4.05 ± 0.02, S 8.66 ± 0.03.

Dehydration of α-ZrP·G, γ-ZrP·G, and ZrSPP·G: The α-**ZrP·G** and **ZrSPP·G** intercalates were dehydrated in a mixture with Al_2O_3 (2 % w/w of the intercalates in Al_2O_3) by heating to 150 °C for 1 h. The γ-**ZrP·G** sample in the same mixture with Al_2O_3 was dehydrated by keeping it in a desiccator over P_2O_5 for 2 d. The intercalates were dehydrated in the mixture with Al_2O_3, because these samples were used directly for the measurement of the UV/Vis spectra. In the following text, the dehydrated samples are denoted as α-**ZrP·G$_D$**, γ-**ZrP·G$_D$**, and **ZrSPP·G$_D$**. To prove the reversibility of the dehydration process, the samples were rehydrated by keeping them over a saturated solution of NaCl, which provides 75 % relative humidity, at room temperature for 3 d.

Characterization Techniques: Powder X-ray diffraction data were obtained with a D8 Advance diffractometer (Bruker AXS, Germany) with a Bragg–Brentano θ–θ geometry (40 kV, 30 mA) by using Cu-K_α radiation with a secondary graphite monochromator. The diffraction angles were measured at room temperature from 2 to 50° (2θ) in 0.02° steps with a counting time of 15 s per step. Diffraction patterns of the dehydrated samples were measured at 150 °C on a heated copper block equipped with a thermocouple. Thermogravimetric measurements (TGA) were performed with use of a home-made apparatus constructed of a computer-controlled oven and a Sartorius BP210 S balance. The measurements were carried out in air between 30 and 960 °C at a heating rate of 5 °C min^{-1}. Infrared spectra in the range of 600–4000 cm^{-1} were recorded at 64 scans per spectrum at a resolution of 2 cm^{-1} by using an HATR adapter with a Perkin–Elmer FTIR Spectrum BX spectrometer on neat samples. All spectra were corrected for the presence of moisture and carbon dioxide in the optical path. UV/Vis diffuse reflectance spectra of the powder materials diluted with Al_2O_3 (up to 2 % w/w) were recorded in the range from 210 to 800 nm with a UV/Vis Lambda 20 spectrometer (Perkin–Elmer, USA) equipped with a diffuse reflectance attachment with a 3 inch integrating sphere with Al_2O_3 as a reference. The reflectance values were recalculated by using the Schuster–Kubelka–Munk equation: $F(R_\infty) = \frac{(1-R_\infty)^2}{2R_\infty}$, where R_∞ is the diffuse reflectance from a semi-infinite layer. Details are given in the previous works.[25]

Molecular Modeling: Molecular mechanics and classical molecular dynamics were carried out in a Materials Studio modeling environment.[26] The unit cell parameters used for the modeling of the host layers were taken from the literature and were the following: α-**ZrP**: a = 9.06 Å, b = 5.297 Å, $\alpha = \gamma$ = 90°, β = 101.71°, space group $P2_1/n$;[27] γ-**ZrP**: a = 5.38 Å, b = 6.64 Å, $\alpha = \gamma$ = 90°, β = 98.69°, space group $P2_1$.[21] We created a two-layered $3a \times 6b \times 2d_{002exp}$ supercell for the α-**ZrP·G** intercalate, in which the composition of one layer was $Zr_{36}(PO_4H)_{72}$. The experimental basal spacings d_{002exp} were 12.2 and 12.0 Å for the hydrated α-**ZrP·G** and dehydrated α-**ZrP·G$_D$** compounds, respectively. In the case of γ-**ZrP·G**, a $6a \times 6b \times 1d_{exp}$ supercell was built, and the composition of the host layer was $Zr_{72}(PO_4H)_{144}$. The experimental basal spacings d_{exp} were 16.3 and 14.6 Å for the hydrated γ-**ZrP·G** and dehydrated γ-**ZrP·G$_D$** compounds, respectively. The number of the guests in the interlayer space was defined on the basis of the experimental measurements, and it was 12 guest molecules per supercell in our models. The model of α-**ZrP·G** contained six guest molecules in each interlayer space, and in the case of γ-**ZrP·G** the interlayer space of the model was filled with 12 guest molecules. The number of the guest molecules in the interlayer space used for the modeling was slightly lower than the amount calculated from the experimental data. Six

molecules of the guest completely filled the interlayer space, and the calculated basal spacings for the models with six guest molecules were in a better agreement with the experimental measurements than models with seven or more guest molecules in one model layer. We suppose that a part of the guests can be also adsorbed on the surface. The experimental results (IR and UV/Vis spectra) showed that the guest can be present in a neutral (unprotonated, **G**) or in a protonated form {as 1*H*-4-[4-(dimethylamino)phenylazo]pyridinium, $\mathbf{G}^+$}. Therefore, we tested two extreme model cases in which the guest molecules were present either as **G** or $\mathbf{G}^+$. In the models containing $\mathbf{G}^+$ cations in the interlayer space, the corresponding amount of the hydrogen atoms was removed randomly from the phosphate groups of the host layer. The negative charge of the host layer thus formed was compensated by the positive charge of the $\mathbf{G}^+$ guest molecules. The initial mutual arrangement of the guests and the arrangement of the guests with respect to the host layer was the same for both the extreme model cases in order to investigate the differences in the arrangement of **G** and $\mathbf{G}^+$. The amount of water was the same in both α-**ZrP** and γ-**ZrP** intercalate hydrates, namely 1.5 H_2O molecules per formula unit, which corresponds to 108 water molecules per supercell. The geometry of the models was optimized in the Universal force field,[28] and the charges were calculated by the Qeq method.[29] The host layers were fixed or treated as rigid units, and the positions of all atoms in the interlayer space were variable. The molecular dynamics was carried out in an *NVT* (*N* = constant number of particles, *V* = constant volume, *T* = constant temperature) canonical statistical ensemble at a temperature of 298 K. The canonical ensemble describes a system in contact with a heat bath. One step of dynamics was 1 fs, and 10^6 steps of dynamics were carried out.

Acknowledgments

The authors thank the Czech Science Foundation (project number 14-13368S) for financial support.

Keywords: Layered compounds · Intercalations · Molecular modeling · Push–pull molecules

[1] M. Ogawa, K. Kuroda, *Chem. Rev.* **1995**, *95*, 399–438.
[2] a) R. Hoppe, G. Alberti, U. Costantino, C. Dionigi, G. Schulz-Ekloff, R. Vivani, *Langmuir* **1997**, *13*, 7252–7257; b) G. G. Aloisi, U. Costantino, F. Elisei, M. Nocchetti, C. Sulli, *Mol. Cryst. Liq. Cryst.* **1998**, *311*, 245–250.
[3] U. Costantino, N. Coletti, M. Nocchetti, G. G. Aloisi, F. Elisei, *Langmuir* **1999**, *15*, 4454–4460.
[4] F. Bureš, *RSC Adv.* **2014**, *4*, 58826–58851.
[5] a) L. R. Dalton, P. A. Sullivan, D. H. Bale, *Chem. Rev.* **2010**, *110*, 25–55; b) M. J. Cho, D. H. Choi, P. A. Sullivan, A. J. P. Akelaitis, L. R. Dalton, *Prog. Polym. Sci.* **2008**, *33*, 1013–1058.
[6] R. Takenawa, Y. Komori, S. Hayashi, J. Kawamata, K. Kuroda, *Chem. Mater.* **2001**, *13*, 3741–3746.
[7] Y. Suzuki, Y. Tenma, Y. Nishioka, J. Kawamata, *Chem. Asian J.* **2012**, *7*, 1170–1179.
[8] a) T. Yi, N. Tancrez, R. Clement, I. Ledoux-Rak, J. Zyss, *J. Lumin.* **2004**, *110*, 389–395; b) Q. M. Liu, W. Zhou, C. Gao, T. Hu, X. J. Zhao, *Chem. Phys. Lett.* **2009**, *477*, 388–391; c) T. Coradin, R. Clement, P. G. Lacroix, K. Nakatani, *Chem. Mater.* **1996**, *8*, 2153–2158.
[9] T. Coradin, R. Backov, D. J. Jones, J. Roziere, R. Clement, *Mol. Cryst. Liq. Cryst.* **1998**, *311*, 275–280.
[10] E. Delahaye, N. Sandeau, Y. Tao, S. Brasselet, R. Clement, *J. Phys. Chem. C* **2009**, *113*, 9092–9100.
[11] a) J. S. O. Evans, S. Benard, P. Yu, R. Clement, *Chem. Mater.* **2001**, *13*, 3813–3816; b) S. Benard, P. Yu, J. P. Audiere, E. Riviere, R. Clement, J. Guilhem, L. Tchertanov, K. Nakatani, *J. Am. Chem. Soc.* **2000**, *122*, 9444–9454.
[12] T. Yi, R. Clement, C. Haut, L. Catala, T. Gacoin, N. Tancrez, I. Ledoux, J. Zyss, *Adv. Mater.* **2005**, *17*, 335–338.
[13] F. Bureš, D. Cvejn, K. Melánová, L. Beneš, J. Svoboda, V. Zima, O. Pytela, T. Mikysek, Z. Růžičková, I. V. Kityk, A. Wojciechowski, N. AlZayed, *J. Mater. Chem. C* **2016**, *4*, 468–478.
[14] a) R. Y. Chen, J. Zhong, C. R. Gu, C. L. Chen, *J. Theor. Comput. Chem.* **2010**, *9*, 861–873; b) G. Alberti, G. M. Lombardo, G. C. Pappalardo, R. Vivani, *Chem. Mater.* **2002**, *14*, 295–303; c) P. Čapková, L. Beneš, K. Melánová, H. Schenk, *J. Appl. Crystallogr.* **1998**, *31*, 845–850.
[15] *International Centre of Diffraction Data*, Swarthmore, PA, USA.
[16] G. Socrates, *Infrared Characteristic Group Frequencies*, John Wiley & Sons, New York, **1997**.
[17] P. L. Stanghellini, E. Boccaleri, E. Diana, G. Alberti, R. Vivani, *Inorg. Chem.* **2004**, *43*, 5698–5703.
[18] J. Bujdák, N. Iyi, T. Fujita, *J. Colloid Interface Sci.* **2003**, *262*, 282–289.
[19] A. Clearfield, U. Costantino in *Layered metal phosphates and their intercalation chemistry* (Eds.: G. Alberti, T. Bein), Pergamon, New York, **1996**, vol. 7, p. 113.
[20] G. Alberti, E. Torraca, *J. Inorg. Nucl. Chem.* **1968**, *30*, 317–318.
[21] D. M. Poojary, B. Shpeizer, A. Clearfield, *J. Chem. Soc., Dalton Trans.* **1995**, 111–113.
[22] V. Zima, J. Svoboda, K. Melánová, L. Beneš, M. Casciola, M. Sganappa, J. Brus, M. Trchová, *Solid State Ionics* **2010**, *181*, 705–713.
[23] R. W. Faessinger, E. V. Brown, *J. Am. Chem. Soc.* **1951**, *73*, 4606–4608.
[24] Y. J. Zhou, R. C. Huang, F. C. Ding, A. D. Brittain, J. J. Liu, M. Zhang, M. Xiao, Y. Z. Meng, L. Y. Sun, *ACS Appl. Mater. Interfaces* **2014**, *6*, 7417–7425.
[25] a) P. Knotek, L. Čapek, R. Bulánek, J. Adam, *Top. Catal.* **2007**, *45*, 51–55; b) R. Bulánek, P. Čičmanec, H. Sheng-Yang, P. Knotek, L. Čapek, M. Setnička, *Appl. Catal. A* **2012**, *415*, 29–39.
[26] *Materials Studio Modeling Environment*, release 4.3, documentation. Accelrys Software Inc., San Diego, CA, **2003**.
[27] J. M. Troup, A. Clearfield, *Inorg. Chem.* **1977**, *16*, 3311–3314.
[28] A. K. Rappé, C. J. Casewit, K. S. Colwell, W. A. Goddard, W. M. Skiff, *J. Am. Chem. Soc.* **1992**, *114*, 10024–10035.
[29] A. K. Rappé, W. A. Goddard, *J. Phys. Chem.* **1991**, *95*, 3358–3363.

Received: August 29, 2016
Published Online: December 7, 2016